

A General Framework to Generate Sizing Systems from 3D Motion Data Applied to Face Mask Design

Timo Bolkart
Saarland University
Saarbrücken, Germany
tbolkart@mmci.uni-saarland.de

Prosenjit Bose
Carleton University
Ottawa, Canada
jit@scs.carleton.ca

Chang Shu
National Research Council
Ottawa, Canada
chang.shu@nrc-cnrc.gc.ca

Stefanie Wuhrer
Saarland University
Saarbrücken, Germany
swuhrer@mmci.uni-saarland.de

Abstract—For the design of mass-produced wearable objects for a population it is important to find a small number of sizes, called a sizing system, that will fit well on a wide range of individuals in the population. To obtain a sizing system that incorporates the shape of an identity along with its motion, we introduce a general framework to generate a sizing system for dynamic 3D motion data. Based on a registered 3D motion database a sizing system is computed for task-specific anthropometric measurements and tolerances, specified by designers. We generate the sizing system by transforming the problem into a box stabbing problem, which aims to find the lowest number of points stabbing a set of boxes. We use a standard computational geometry technique to solve this; it recursively computes the stabbing of lower-dimensional boxes. We apply our framework to a database of facial motion data for anthropometric measurements related to the design of face masks. We show the generalization capabilities of this sizing system on unseen data, and compute, for each size, a representative 3D shape that can be used by designers to produce a prototype model.

Keywords—design models; face mask design; 3D face modeling

I. INTRODUCTION

Face masks and respirators exist in many different types and sizes and are widely used, by the military (e.g. for pilots' oxygen masks [1]), by public safety departments (e.g. respirators for firefighters [2]), and for medical (e.g. aerosol face masks [3]) and automotive applications (e.g. paint respirators). Depending on the type of face mask, it is designed to supply oxygen or filter air. For most kinds of face masks it is important to fit many different kinds of face shapes. Leakage could cause, for aerosol face masks, a contamination of the caregiver's area, and for respirators, an inhalation of harmful gases and particles, which could cause lung diseases or other health problems. Furthermore, loosely fitting oxygen masks with leakage towards the eyes are uncomfortable to wear. A tight fit without leakage is therefore crucial for the design of an effective face mask.

In ergonomics, many works exist that aim at creating sizing systems based on anthropometric measurements for the design of face masks [3], [1], [2], [4], helmets [5], gloves [6] or more general, for apparel [7]. The aim of generating a sizing system for a population with a low

number of different sizes is that a designed product fits a wide range of individuals in the population. To generate a sizing system, design-specific anthropometric measurements are gathered for a population and groups are formed, where identities with similar measurements are within the same group. Each group is then represented by a size within the sizing system.

In computer vision, many works focus on human faces due to the wide variety of potential applications, such as entertainment or security. Due to the availability of several 3D face databases (e.g. [8], [9], [10], [11]), statistical methods are widely used to analyze the facial shape and its variations across different identities and different expressions. These statistical methods are used for various tasks, e.g. to reconstruct 3D faces from low-dimensional data like 2D images [12] or to compute animations of 3D faces given static face scans [13].

Further applications of statistical methods are in ergonomic design, e.g. to study the influence of shape variations for the design of face masks [14], [15]. Furthermore, 3D face databases can be used to generate sizing systems for anthropometric measurements extracted from a registered static face database [5].

Currently, the design of face masks only considers the shape of neutral faces. Since face masks are worn for long periods, it is likely that a wearer will move his or her face while wearing the mask, e.g. by talking or changing facial expressions. Therefore, a tight fit of the face mask is also necessary in the presence of facial motion, to avoid leakage caused by motion.

We introduce a general framework to generate a sizing system for any kind of 3D motion data. 3D motion data in this context are databases that contain sequences of 3D scans of the same class of object (e.g. human faces or bodies). This database contains data of different identities, each performing one or more motion sequences consisting of an arbitrary number of frames. All shapes in these sequences need to be in full correspondence.

Given a registered motion database, the input for our framework is the specification of the anthropometric measurements used. Furthermore, an ordered set of tolerances

must be specified for each dimension, and the number of sizes that should be computed must be given (otherwise a sizing system is found that fits for all input data). These input parameters are specific for the designed product and must be specified by designers. Given these parameters, our framework outputs a sizing system with the specified number of sizes, together with representative 3D shape models for each size.

Given a set of problem-specific anthropometric measurements, each shape in the database of 3D motion data is represented by a point in high-dimensional parameter space. A sizing system is then computed by solving a stabbing problem in parameter space.

Our contributions are

- A general framework to generate a sizing system for dynamic 3D motion data.
- Generation of a representative 3D model for each size for fabrication.
- Application of our framework to generate a specific sizing system for facial motion data.

Our framework is independent of the kind of data and the type of measurements. While our method is able to compute a sizing system for a set of anthropometric measurements without a given registered motion database, for the computation of a representative 3D shape for each size, the registered database is needed.

Leveraging tools and datasets developed by the 3D vision and graphics communities for automated design systems has the potential to improve design processes and lead to safer and more comfortable products.

II. RELATED WORK

Our work is most related to works in ergonomic design that aim at generating sizing systems for faces. Amirav et al. [3] improve the design of aerosol face masks for infants based on two anthropometric measurements taken from 3D face scans. They cluster the set of measurements, compute representative 3D face shapes for each cluster and use these to fabricate face masks. Lee [1] classifies the importance of anthropometric facial measurements for the design of oxygen masks. Based on two measurements, he computes a sizing system for the design of oxygen masks for Korean air force pilots. Han et al. [4] use ten anthropometric measurements from 3D face scans for the design of face masks. They compute a sizing system by splitting each measurement dimension independently into three groups. In contrast to our approach, these methods cannot be used to generate a sizing system considering design-specific tolerances. Furthermore, none of these methods can be applied for dynamic motion data.

Moreover, methods exist that are not directly applied to the design of face masks, even though they potentially could be. McCulloch et al. [7] and Wuhner et al. [5] propose methods that compute general sizing systems for

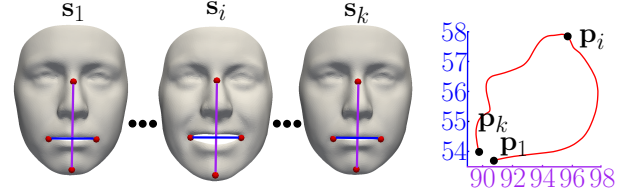


Figure 1. Representation of the anthropometric measurements face length (purple) and lip width (blue) for motion sequence. Left: 3D motion sequence. Right: Resulting curve in parameter space.

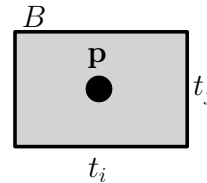


Figure 2. Given some tolerances t_i and t_j and some gear designed for measurements represented by a point \mathbf{p} in parameter space, all points within a parameter box B centered at \mathbf{p} are fit by the gear.

anthropometric data. McCulloch et al. define a distance function that measures the distance of measurements from the sizing system and the measurements taken from the database. To get a good fitting system, they perform a non-linear optimization. Wuhner et al. generate a sizing system with fixed sizes by solving a box-covering problem for arbitrary anthropometric measurements. While both methods are able to compute a sizing system with a fixed number of sizes, and furthermore are able to operate in an arbitrary dimensional parameter space, they are not applicable for dynamic motion data.

To the best of our knowledge, our method is the first one generating a sizing system in any number of dimensions for dynamic motion data.

Another body of work statistically analyzes the shape of the face and studies its influences on the design of face masks. Zhuang et al. [14] and Luximon et al. [15] analyze the facial shape by computing principal component analysis (PCA) on a set of facial landmarks for datasets of 3D faces. Zhuang et al. discuss the potential influence of learned variations for the design of respirators, Luximon et al. the influence on the design of face masks and eyewear.

Also related to our work are methods that capture databases of 3D faces in motion. Databases that capture dynamic 3D faces are e.g. BU-4DFE [10] and D3FACS [11]. The BU-4DFE database captures motion data of 101 subjects of different ethnicities performing six different expressions over time. The D3DFACS database captures, for 10 subjects, several different Action Units from the Facial Action Coding System. Our goal is to compute a sizing system for a dynamic motion database. We apply our framework to registered sequences of the BU-4DFE database.

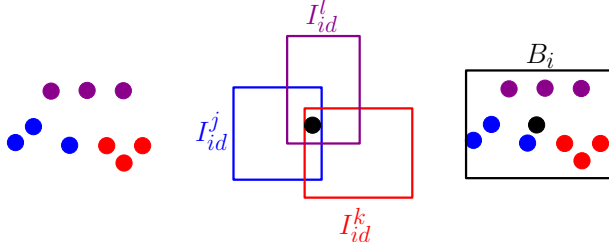


Figure 3. Computation of box covering using box stabbing. Left: Multiple points in parameter space from different identities (one color per identity) that should be covered. Center: Identity boxes together with a stabbing point (black). Right: Parameter box centered at the computed stabbing point that covers all points of different identities.

III. PARAMETER SPACE FOR DYNAMIC MOTION DATA

In this section, we introduce a parameter space of anthropometric measurements for dynamic data, and describe a method to fully automatically compute a sizing system for this parameter space. Given a database of 3D faces in motion in full correspondence, we extract an ordered set of d anthropometric measurements from each scan. For each scan \mathbf{s}_i of a motion sequence, the set of measurements is denoted by $\mathbf{p}_i \in \mathbb{R}^d$. The set of all measurements of all scans defines the high-dimensional parameter space $\mathbb{P} \subseteq \mathbb{R}^d$. Since each frame of a motion sequence gives a point in \mathbb{P} , an entire sequence is represented by a curve in \mathbb{P} . Figure 1 shows two measurements extracted from a motion sequence, resulting in a curve in \mathbb{P} . Since for each identity, multiple motion sequences may exist, one identity is represented by a set of curves, one for each motion sequence.

The designer can specify a tolerance t_i along each dimension i that specifies the amount of stretch supported by the specific gear. For the specified tolerances, a d -dimensional axis-aligned parameter box B is defined, where the length of the side in dimension i is t_i . Some gear designed to fit for some measurements $\mathbf{p} \in \mathbb{P}$ therefore also fits to all points in \mathbb{P} within a translated copy of B centered at \mathbf{p} (see Figure 2). A sizing system can then be computed by covering the parameter space using translated copies B_i of B . Since our goal is to design a sizing system for motion data, where the gear fits for an identity through various motions, all curves of one identity must be contained within the same box B_i .

IV. COVERING OF PARAMETER SPACE USING BOX STABBING

All curves of one identity need to be covered by the same box. The greedy box covering method by Wuhler et al. [5] repeatedly selects the box centered at a point in parameter space that covers the most uncovered points. This greedy covering method cannot be applied to dynamic data, since a box centered at one point does not necessarily cover all curves of the identity.

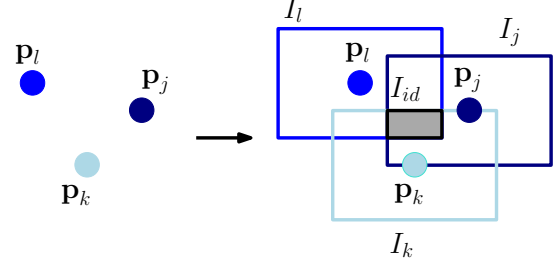


Figure 4. Computation of the identity box I_{id} for points of one identity. The box I_{id} bounds the area, where each point chosen as center of B_i covers all points of the identity in parameter space.

Instead, we transform the problem into a d -dimensional stabbing problem as shown in Figure 3. First, we compute, for each identity, the area I_{id} , where a box B_i can be centered to cover all curves of that identity. Figure 4 shows the construction of I_{id} for three selected points of one identity. For each point \mathbf{p}_i from one identity (for one identity, each frame of each motion sequence is represented by $\mathbf{p}_i \in \mathbb{P}$) we define I_i to be the area within a copy of B , centered at \mathbf{p}_i . By construction, any B_i with center within I_i contains \mathbf{p}_i . We obtain I_{id} by intersecting all I_i of one identity. For each identity the area I_{id} defines a region where each point chosen as the center of B_i covers all points \mathbf{p}_i belonging to one identity. If a point within the intersection of multiple I_{id} is chosen as the center of B_i , B_i contains multiple identities.

To get a covering of the parameter space we now search for the minimum set of points such that each I_{id} is stabbed by at least one point. Each stabbing point represents the center of a cover box in parameter space. We use the method by Nielson [16] to compute this stabbing.

A. Full Stabbing of Dynamic Identity Boxes

To compute the optimal stabbing of 1-dimensional intervals and axis-parallel d -dimensional boxes, Nielson [16] proposes two divide-and-conquer algorithms. While the 1-dimensional stabbing can be solved optimally, computing a d -dimensional stabbing for $d \geq 2$ is NP-complete. The proposed algorithm to compute the d -dimensional stabbing gives a bounded approximation of the optimal solution.

To get an optimal 1-dimensional stabbing, the rightmost lower interval point is selected and all intervals that are stabbed by this point are removed. This is repeated until all intervals are stabbed. This stabbing is computed using the following output-sensitive algorithm. The input set of n intervals I is recursively split into right and left subsets of intervals, with respect to the median of all lower interval endpoints. If a subset contains only one interval, the lower endpoint of the interval is chosen as a stabbing point. All intervals stabbed by the chosen stabbing point are removed from further processing. The algorithm stops once all intervals are stabbed. The time complexity of this stabbing is

$\Theta(n \log c^*(I))$, where $c^*(I)$ denotes the minimum number of stabbing points necessary to stab all intervals.

To compute a stabbing of a set I of n d -dimensional axis-parallel boxes, the input set of boxes is separated into three subsets. For dimension d of the boxes, a stabbing is computed for the 1-dimensional intervals and the median stabbing point is used to separate the input set of boxes into three subsets: all boxes that intersect the median stabbing point, the subsets to the left, and the subset to the right of the median stabbing point. The right and left subsets are then recursively separated into three subsets. For the intersecting subset, the stabbing median value is fixed for dimension d and the stabbing of the $(d - 1)$ -dimensional boxes is computed recursively. The method outputs $c(I)$ points in time $O(dn \log c(I))$, where $c(I) \leq b^*(I)(1 + \log_2 b^*(I))^{d-1}$ with $b^*(I)$ is the maximum number of pairwise disjoint boxes.

B. Stabbing with a Fixed Number of Points

For the design of wearables for large populations, it is not desirable to create a sizing system with a large number of different sizes that fits the entire population. Instead, a sizing system with a fixed number of sizes that fit the maximum number of individuals is sought. We therefore search for a fixed number of stabbing points that stab the maximum number of identity boxes. We use a greedy approach to solve this. We first compute the full stabbing of the parameter space using the method described in Section IV-A. We then iteratively select the stabbing points that stab the most unstabbed identity boxes.

V. REPRESENTATION OF COVERING

After computing a sizing system for the parameter space, we aim at computing a representative 3D face model for each of the sizes. This representative face model can be used for fabrication. One possibility is to compute the full Procrustes mean [17] of all identities covered by the box. To compute the full Procrustes mean of a set of shapes in correspondence, we iteratively compute the mean over all shapes, and each of the shapes is rigidly aligned to the mean shape. This is also used by Wuhrer et al. [5] to compute a representative model.

Another possibility is to select the model that is closest in parameter space to the cover box center as used by Han et al. [4] and Lee [1]. For data that are dense in parameter space, the model closest to the cover box center is expected to give a good representation of the box.

A further method to compute a representative model for the cover box is feature analysis by Allen et al. [18] as used by Wuhrer et al. [5]. Wuhrer et al. compute a linear mapping between the parameter space and a linear PCA space of 3D faces to reconstruct 3D faces for given sets of measurements in parameter space. In contrast to our approach, their method only uses faces in one neutral expression, and the variations

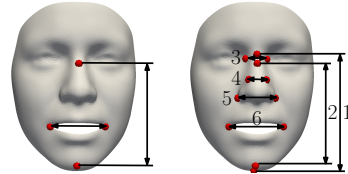


Figure 5. Important measurements for face mask design. Left: Two important measurements for the design of aerosol face masks [3]. Right: Six measurements classified as being of high importance for the design of oxygen masks [1].

of the data can therefore be modeled using a linear PCA model. Since our data contain variation due to motion and shape differences of different identities, the variations cannot be modeled using a linear space. Therefore, a linear mapping between the parameter space and the non-linear model space does not lead to representative 3D face models.

VI. EVALUATION

This section evaluates the proposed space covering using measurements associated with the design of face masks. The motion data are from the BU-4DFE database [10], which contains the motion data of 101 identities performing six expressions (anger, disgust, fear, happiness, sadness, surprise) over time. The motion database is registered using the method described by Bolkart and Wuhrer [13]. There, an entire motion sequence is registered using a multilinear model as statistical prior. Based on the temporal registration of the motion sequences, we choose five representative frames of each sequence that cover the full range of motion. In the following, each sequence is therefore represented by five points in parameter space.

In our experiments we show how well the computed sizing system fits for a given dataset, and its generalization to unseen data. To this end, we randomly divide the motion sequences into a training and a test set, each containing about 50% of the data, with the same ratio of male and female subjects. For our experiments we do not consider the surprise facial expression, since many of the surprise motion sequences are performed in an artificial fashion by fully opening the mouth, which we think would be an unnatural behavior for a person wearing a face mask. Hence, for each identity up to five motion sequences are used, which gives us up to 25 points in parameter space for each identity. Overall we use 390 dynamic motion sequences from 98 identities.

A. Anthropometric Measurements for Face Mask Design

For the design of face masks, different measurements are important, depending on the type of mask and its application area. Amirav et al. [3] use two measurements (at left in Figure 5) for the design of aerosol face masks. Lee [1] classifies 22 facial measurements according to their importance for the design of oxygen masks. The six facial measurements shown at right in Figure 5 are classified as

Measurement	Face length	Lip width
Mean	10.87	8.05
Standard deviation	3.35	3.05
Median	10.98	8.08
Maximum	19.43	14.40

Table I

STATISTICS IN MM COMPUTED OVER THE MAXIMUM MEASUREMENT RANGE OVER ALL IDENTITIES FOR THE 2D PARAMETER SPACE (FOR MEASUREMENTS SEE LEFT OF FIGURE 5).

Measurement	1	2	3	4	5	6
Mean	10.47	10.87	1.47	1.07	4.68	8.05
Standard deviation	3.32	3.35	0.56	0.50	1.80	3.05
Median	10.2	10.98	1.52	1.02	4.66	8.08
Maximum	18.59	19.43	2.91	2.34	8.28	14.40

Table II

STATISTICS IN MM COMPUTED OVER THE MAXIMUM MEASUREMENT RANGE OVER ALL IDENTITIES FOR THE 6D PARAMETER SPACE (FOR MEASUREMENTS SEE RIGHT OF FIGURE 5).

being of high importance for oxygen masks. We use two different sets of measurements to evaluate our approach: first, the two measurements used by Amirav et al. leading to a 2D parameter space, and second, the six measurements by Lee, leading to a 6D parameter space.

B. Dynamic Data Analysis

This section evaluates the variations within the training data caused by motion. For each identity, we compute the axis-aligned bounding box covering all points in parameter space. This axis-aligned bounding box is computed as the difference of maximum and minimum values along each measurement dimension over all points of the identity in parameter space. For each identity the axis-aligned bounding box is the smallest possible parameter box that is able to cover the identity. Since for static data each identity consists of only a single point in parameter space, the side length of an axis-aligned bounding box for static data would be zero. The side length of the box measures the influence of the motion for dynamic motion data. We analyze the variation of the measurements due to motion by computing mean, standard deviation, median and maximum of the side lengths of the axis-aligned bounding boxes over all identities (see Table I for the 2D parameter space, and Table II for 6D, respectively). For both tables, the maximum values describe the minimum parameter box size necessary for a full covering of the parameter space to be computed.

C. Space Covering of Training Data

Given a fixed number of boxes, we want to get a good covering of the parameter space of the training data. We therefore choose the tolerances for the size of the box B based on the analysis of the training data from Section VI-B. For the covering of the 2D parameter space (at left in

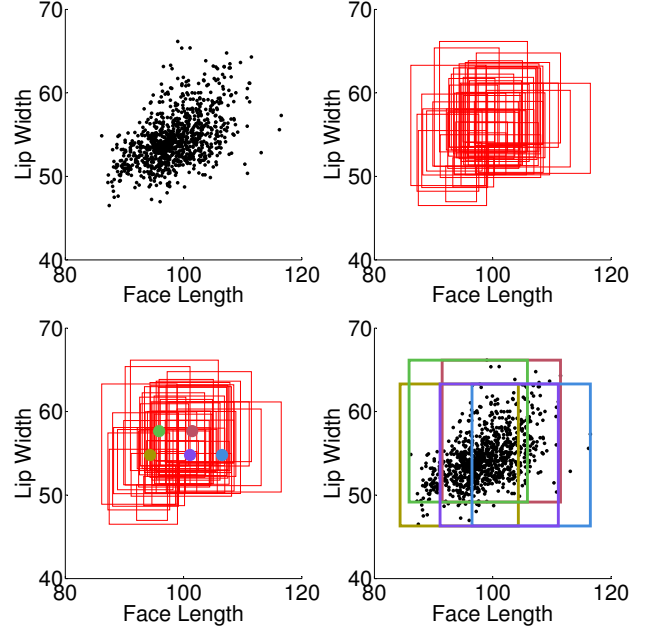


Figure 6. Overview of our parameter space covering approach. Upper left: Points in 2D parameter space. Upper right: Computed identity boxes I_{id} . Lower left: Full stabbing of identity boxes with 5 stabbing points. Lower right: Resulting covering in parameter space.

Space dimension	3 boxes	5 boxes
2D	94.0	100.0
6D	74.0	82.0

Table III

PERCENTAGE OF COVERED TRAINING DATA WITH A FIXED NUMBER OF PARAMETER BOXES FOR 2D AND 6D PARAMETER SPACE.

Figure 5) we choose tolerances of 20 mm for the face length and 17 mm for the lip width. Figure 6 shows the different steps of our covering method for the training data. The upper left of Figure 6 shows the training data in parameter space, where each identity is represented by up to 25 points. The upper right shows the identity boxes computed as described in Section IV. The lower left then shows the stabbing points for the identity boxes from Section IV-A. The lower right shows the resulting covering. For the covering of the 6D parameter space, spanned by the measurements at right in Figure 5, we choose the tolerances 1 = 20 mm, 2 = 20 mm, 3 = 5 mm, 4 = 5 mm, 5 = 10 mm, and 6 = 17 mm.

For both parameter spaces, we compute a covering with three and five boxes and measure the number of identities that are fully covered by these boxes (see Table III). With three boxes, 94% of the identities in 2D parameter space are covered, and 74.0% of the 6D parameter space. With five boxes, all identities of the 2D parameter space are covered, and 82.0% of the 6D parameter space. Since for the 6D case the same number of points is embedded in a higher-dimensional parameter space, it is expected that more boxes

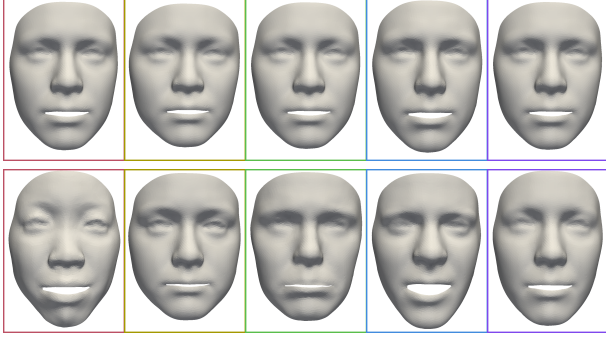


Figure 7. Representation of the motion space covering. Top: Procrustes mean shape for the five cover boxes for the 2D parameter space of the training data. Bottom: Faces from the training data closest to the box center in parameter space for the 2D parameter space of the training data.

Space dimension	3 boxes	5 boxes
2D	81.4	91.7
6D	58.3	64.6

Table IV

GENERALIZATION OF THE COVERING. PERCENTAGE OF COVERED TEST DATA WITH THE COVERING COMPUTED FOR THE TRAINING DATA FOR 2D AND 6D PARAMETER SPACE.

are needed to cover the full space and that the same number of boxes cover a lower percentage of the data. Computing the full covering of both parameter spaces takes less than a second, running on a standard PC.

For each of the computed 2D cover boxes, we compute representative 3D face shapes as described in Section V. First, for each box, we compute the full Procrustes mean over all identities fully covered by the box. The top of Figure 7 shows the full Procrustes mean for the five 2D cover boxes. Computing the full Procrustes mean leads to a good representation if the mean of the shapes used for computation is close to the box center. For our dynamic motion data a large amount of variation in parameter space is caused by the motion rather than by shape differences between different identities. Since identities need to be fully covered by boxes, the sizes of the boxes need to be large for data with large motion variations. With large boxes the overlap between different boxes is also large, and some identities are covered by multiple boxes. This causes the Procrustes mean shapes of different boxes to be similar.

Second, we find, for each box, the shape within the training database that is closest to the center of the box in parameter space. The bottom of Figure 7 shows the face shapes closest to the box centers in parameter space. Compared to the Procrustes mean shape, they are more distinctive and give a representative 3D geometry for the boxes.

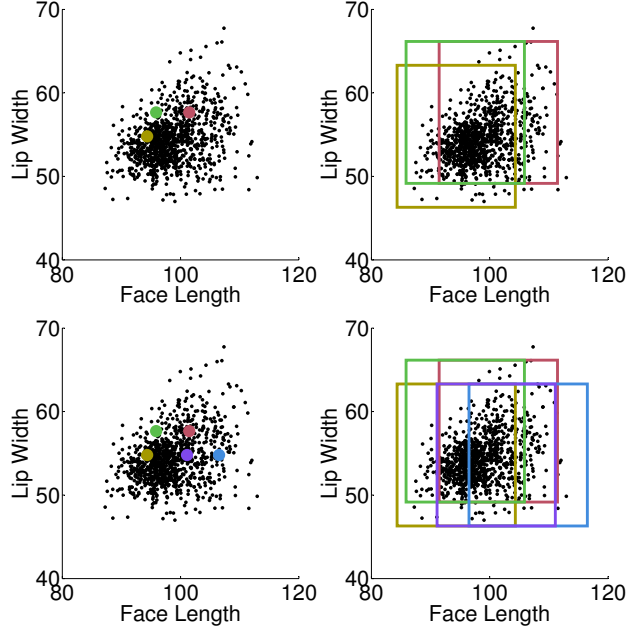


Figure 8. Covering applied to unseen data. Upper left: Midpoints of first three greedily selected cover boxes (stabbing points). Upper right: First three greedily selected cover boxes. Lower left: Midpoints of full training covering (stabbing points). Lower right: Full training covering.

D. Generalization of Space Covering

In this section we evaluate how well the space covering computed for the training data from Section VI-C generalizes to unseen data. Figure 8 shows in 2D parameter space the covering computed on the training data applied to the test data. The top row of Figure 8 shows the first three greedily selected stabbing points (left) and cover boxes (right), the bottom row shows the stabbing points (left) and cover boxes (right) of the full training covering.

To compute the generalization ability, we check, for each identity of the test data, whether it is fully covered by one of the training parameter boxes. An identity is fully covered by a parameter box if for that identity, all its points in parameter space are within the same box. Table IV shows the covering rates for the test data. For three cover boxes, 81.4% of the test data identities are covered in 2D parameter space, and 58.3% in 6D parameter space. For five cover boxes, 91.7% of the test data identities are covered in 2D parameter space, and 64.6% in 6D parameter space. As for the covering of the training data, it is expected that the same number of boxes covers a lower percentage of the data in 6D than in 2D.

VII. LIMITATIONS

While the sizing system computation in our framework is generally applicable for all kinds of measurements, our overall framework has some limitations. Since the computation of a 3D face representation requires a registered database, facial hair, or other partial occlusions caused by glasses, are not accounted for by our framework.

Furthermore, we assume the tolerances for each measurement dimension to be independent and therefore form a box in parameter space. If the tolerances are not independent, e.g. they form any other convex shape I_i in parameter space covering \mathbf{p}_i , the region I_{id} for each identity is given by an arbitrary-shaped convex object (intersection of I_i of all points). To obtain a sizing system for these tolerances, we would need to compute the stabbing of arbitrary-shaped convex shapes.

Producing a real prototype of a face mask based on our computed sizing system for dynamic data together with a user study to evaluate its quality in a real-world application is left for future work.

VIII. CONCLUSION

In this work, we proposed a general framework to compute a sizing system for dynamic motion data. We compute a covering of the low-dimensional parameter space with translated copies of a box of fixed size, defining the tolerances of a designed product along each measurement dimension. The covering is computed using a d -dimensional box stabbing method. We apply our framework to sets of anthropometric measurements used for the design of face masks, and evaluate our sizing system in terms of its ability to fit unseen data. For each size of the sizing system created, we compute a representative 3D geometry that can be used by designers to produce a prototype model.

ACKNOWLEDGMENTS

This work has been funded by the Cluster of Excellence on *Multimodal Computing and Interaction* within the Excellence Initiative of the German Federal Government.

REFERENCES

- [1] W. Lee, "Development of a design methodology of pilot oxygen mask using 3D facial scan data," Ph.D. dissertation, Pohang University of Science and Technology, Korea, 2013.
- [2] M. A. Balkhyour, "Evaluation of full-facepiece respirator fit on fire fighters in the municipality of Jeddah, Saudi Arabia," *International Journal of Environmental Research and Public Health*, vol. 10, no. 1, pp. 347–360, 2013.
- [3] I. Amirav, A. S. Luder, A. Halamish, D. Raviv, R. Kimmel, D. Waisman, and M. T. Newhouse, "Design of aerosol face masks for children using computerized 3D face analysis," *Journal of Aerosol Medicine and Pulmonary Drug Delivery*, vol. 26, no. 0, pp. 1–7, 2013.
- [4] D.-H. Han, J. Rhi, and J. Lee, "Development of prototypes of half-mask facepieces for Koreans using the 3D digitizing design method: A pilot study," *Annals of Occupational Hygiene*, vol. 48, no. 8, pp. 707–714, 2004.
- [5] S. Wuhrer, C. Shu, and P. Bose, "Automatically creating design models from 3D anthropometry data," *Journal of Computing and Information Science in Engineering*, vol. 12, no. 4, pp. 1–7, 2012.
- [6] O. Kwon, K. Jung, H. You, and H.-E. Kim, "Determination of key dimensions for a glove sizing system by analyzing the relationships between hand dimensions," *Applied Ergonomics*, vol. 40, no. 4, pp. 762 – 766, 2009.
- [7] C. E. McCulloch, B. Paal, and S. P. Ashdown, "An optimisation approach to apparel sizing," *The Journal of the Operational Research Society*, vol. 49, no. 5, pp. pp. 492–499, 1998.
- [8] L. Yin, X. Wei, Y. Sun, J. Wang, and M. J. Rosato, "A 3D facial expression database for facial behavior research," in *IEEE International Conference on Automatic Face and Gesture Recognition*, 2006, pp. 211–216.
- [9] A. Savran, N. Alyuz, H. Dibeklioglu, O. Celiktutan, B. Gökberk, B. Sankur, and L. Akarun, "Bosphorus database for 3D face analysis," in *Biometrics and Identity Management*, 2008, pp. 47–56.
- [10] L. Yin, X. Chen, Y. Sun, T. Worm, and M. Reale, "A high-resolution 3D dynamic facial expression database," in *IEEE International Conference on Automatic Face and Gesture Recognition*, 2008, pp. 1–6.
- [11] D. Cosker, E. Krumhuber, and A. Hilton, "A FACS valid 3D dynamic action unit database with applications to 3D dynamic morphable facial modeling," in *IEEE International Conference on Computer Vision*, 2011, pp. 2296–2303.
- [12] V. Blanz and T. Vetter, "A morphable model for the synthesis of 3D faces," in *SIGGRAPH*, 1999, pp. 187–194.
- [13] T. Bolkart and S. Wuhrer, "Statistical analysis of 3D faces in motion," in *3D Vision*, 2013, pp. 103–110.
- [14] Z. Zhuang, D. Slice, S. Benson, D. Landsittel, and D. Viscusi, *Digital Human Modeling*. Springer Berlin Heidelberg, 2009, ch. Facial Shape Variation of U.S. Respirator Users, pp. 578–587.
- [15] Y. Luximon, R. Ball, and L. Justice, "The Chinese face: A 3D anthropometric analysis," *International Symposium on Tools and Methods of Competitive Engineering*, vol. 1, pp. 255–265, 2010.
- [16] F. Nielsen, "Fast stabbing of boxes in high dimensions," *Theoretical Computer Science*, vol. 246, no. 12, pp. 53 – 72, 2000.
- [17] I. Dryden and K. Mardia, *Statistical shape analysis*. Wiley, 1998.
- [18] B. Allen, B. Curless, and Z. Popović, "The space of human body shapes: reconstruction and parameterization from range scans," *ACM Transactions on Graphics (Proc. SIGGRAPH)*, vol. 22, no. 3, pp. 587–594, 2003.